Published in final edited form as:
Magn Reson Med. 2008 May ; 59(5): 1165–1169. doi:10.1002/mrm.21574.

Regional Metabolite T_2 in the Healthy Rhesus Macaque Brain at 7T

Songtao Liu[1], **Oded Gonen**[1,*], **Lazar Fleysher**[1], **Roman Fleysher**[1], **Brian J. Soher**[2], **Sarah Pilkenton**[3], **Margaret R. Lentz**[3], **Eva-Maria Ratai**[3], and **R. Gilberto González**[3]

1*Department of Radiology, New York University School of Medicine, New York, New York, USA.*

2*Center for Advanced MR Development, Department of Radiology, Duke University Medical Center, Durham, North Carolina, USA.*

3*Massachusetts General Hospital, A.A. Martinos Center for Biomedical Imaging and Neuroradiology Division, Charlestown, Massachusetts, USA.*

Abstract

Although the rhesus macaque brain is an excellent model system for the study of neurological diseases and their responses to treatment, its small size requires much higher spatial resolution, motivating use of ultra-high-field (B_0) imagers. Their weaker radio-frequency fields, however, dictate longer pulses; hence longer TE localization sequences. Due to the shorter transverse relaxation time (T_2) at higher B_0s, these longer TEs subject metabolites to T_2-weighting, that decrease their quantification accuracy. To address this we measured the T_2sof *N*-acetylaspartate (NAA), choline (Cho), and creatine (Cr) in several gray matter (GM) and white matter (WM) regions of four healthy rhesus macaques at 7T using three-dimensional (3D) proton MR spectroscopic imaging at $(0.4\ \text{cm})^3 = 64$ μl spatial resolution. The results show that macaque T_2s are in good agreement with those reported in humans at 7T: 169 ± 2.3 ms for NAA (mean ± SEM), 114 ± 1.9 ms for Cr, and 128 ± 2.4 ms for Cho, with no significant differences between GM and WM. The T_2 histograms from 320 voxels in each animal for NAA, Cr, and Cho were similar in position and shape, indicating that they are potentially characteristic of “healthy” in this species.

Keywords

animal models; MR spectroscopic imaging; rhesus macaque; transverse relaxation time; brain metabolites, 7 Tesla

Since the brain of nonhuman primates is biochemically, morphologically, and functionally similar to its human counterpart, rhesus macaques are increasingly used as advanced models for disease and treatment studies, e.g., in neuroAIDS (1), ischemic stroke (2), and Parkinson's and Huntington's diseases (3). Due to the need for repeated measurements, these studies favor nondestructive means: MRI for morphology and function, and proton MR spectroscopy (^{1}H-MRS) for assessment of neuronal cells, cell energetics, and membrane turnover, through the levels of their surrogate markers, *N*-acetylaspartate (NAA), creatine (Cr), and choline (Cho) (4,5).

Unlike MRI, in which anatomy or contrast can be evaluated visually, ^{1}H-MRS requires measurement of additional parameters for quantitative assessment. While instrumental factors (e.g., static, B_0, and radio frequency [RF] field [B_1] inhomogeneity) can be handled by field mapping (6), line fitting (7), and internal water referencing (8), molecular environment factors

*Correspondence to: Oded Gonen, Department of Radiology, New York University School of Medicine, 650 1st Avenue 6th floor, New York, NY 10016. E-mail: oded.gonen@med.nyu.edu.

require knowledge of local longitudinal (T_1) and transverse (T_2) relaxation times (4). Although T_1- and T_2-weighting can be reduced with long repetition and short echo-times (TR $\gg$ T_1 and TE $\ll$ T_2) intermediate- and long-TE spectra are often preferred for their flatter baseline, decreased lipid contamination, and simpler peak structure (4). Consequently, reliable estimation of the metabolites' T_2 values is needed for their accurate quantification, especially at high fields (9,10).

MRS in animal models is most relevant if voxels can be assigned to analogous human structures. Given that the ~80 cm^3 macaque brain is 16-fold smaller than the average human's 1250-cm^3 brain (11,12), isotropic (1.0 cm)^3 voxels in the latter scale to (0.4 cm)^3 = 64 μl in the former and since the signal-to-noise-ratio (SNR) depends only on voxel size and acquisition time (13), such resolution favors higher B_0s. Unfortunately, the lower RF power available at the higher B_0s (typically 5−8 kW at 7T vs. up to 30 kW at 3T) also produce less B_1 (half as much at 7T than at 4T) per Watt (14), limiting the power that can be delivered to the coil before voltage breakdown or power deposition (specific absorption rate [SAR]) limits are exceeded, even in animals. A simple way to avoid both issues is to extend the duration of the RF pulses (and consequently the TE) in order to reduce their peak amplitude. The shorter T_2s at higher B_0, however (15,16), may render such sequences "intermediate" or "long" TE that subject metabolites to unknown T_2-weighting (4).

Regional in vivo metabolite level variations make three-dimensional (3D) MR spectroscopic imaging (MRSI) the localization method of choice (5). To facilitate correction for the adverse effect of T_2-weighting on the accuracy of metabolic quantification we measured the T_2s of NAA, Cho, and Cr in several brain regions of four rhesus macaques at 7T with 3D MRSI at 64 μl spatial resolution using a two-point protocol optimized for precision per unit time (17).

MATERIALS AND METHODS

Nonhuman Primates

A total of four (two male, two female) healthy, 6- to 10-kg, 9- to 13-year-old, adult rhesus macaques (*Macaca mulatta*) were studied. Each was tranquilized with 15−20 mg/kg ketamine hydrochloride (intramuscular) and intubated to ensure a patent airway during the experiment (no mechanical ventilation was needed). Intravenous injection of 0.4 mg/kg atropine was administered to prevent bradycardia. Continuous infusion of 0.25 mg/kg/min propofol was maintained throughout via catheter in a saphenous vein. Heart rate, oxygen saturation, end-tidal CO_2, and respiratory rate were continuously monitored. A heated water blanket and rectal temperature monitor were used to prevent hypothermia. Animals were under constant veterinary supervision and the protocol was approved by the Harvard Medical School and Massachusetts General Hospital (MGH) Institutional Animal Care and Utilization Committee (IACUC).

Instrumentation and MRI

All experiments were done in a 7T Magnetom imager (Siemens AG, Erlangen, Germany) with 18 cm × 18 cm diameter × depth transmit-receive head-coil (MR Instruments, Minneapolis, MN, USA). The coil produces up to 1 kHz B_1 at 297 MHz with ~2.4 kW reaching it from the 5-kW power amplifier. To image-guide the ^{1}H-MRS volume of interest (VOI), sagittal, coronal, and axial turbo spin-echo MRI images were acquired at: TE/TR = 13 ms/5000 ms, matrix size = 512 × 521, 160 × 160 mm^2, and slice thickness = 2 mm, as shown in Fig. 1.

^{1}H-MRSI

Our chemical-shift imaging (CSI)-based procedure adjusted the first and second order shims to consistent 65 ± 5 Hz whole-head water linewidth. A 40 × 32 × 16 mm^3 anterior-posterior ×

left-right × inferior-superior (AP × LR × IS) VOI was image-guided onto the anatomy of interest and aligned along the splenium-genu axis of the corpus callosum (see Fig. 1). Manual shimming reduced the water linewidth to 50 ± 5 Hz. The VOI was excited using point-resolved spectroscopy sequence (PRESS) (TR = 1600 ms, see choice of TEs below) with two interleaved second-order Hadamard-encoded slabs (four slices) for optimal duty-cycle and SNR (18). This also allows us to double the Hadamard slice-select gradient to 12 mT/m for minimal 0.7 mm (17.5% slice width) chemical-shift displacement between NAA and Cho. These slices were 16 × 16 (LR × AP) 2D CSI-encoded in a 64 × 64 × 16 mm^3 (AP × LR × IS) FOV to yield 320 isotropic (0.4 cm^3) voxels in the VOI. Signals were digitized for 256 ms with 2048 complex points at a bandwidth = 4 kHz. Each 3D ^{1}H-MRSI "block" was acquired in 13.7 min.

Choice of TE and Acquisition Strategy

The desire for higher spatial resolution and T_2 precision in the noisy MRSI experiment makes for long acquisition times. To maximize its efficiency we employed two strategies: 1) 3D ^{1}H-MRSI that yields the same SNR per given time as single-voxel methods (13) yet covers a much larger volume (18); and 2) a two-point scheme that optimizes not just the usual two TEs, but also the number of averages (N_1 and N_2) at each TE, for the best T_2 estimate/unit time (9,17). Using the literature human Cr T_2^0 of ≈ 100 ms (15) as the initial "guess" for the T_2s sought, has led to TE_1 = 39 ms (minimum for our setup), N_1 = 4, and TE_2 = 165 ms ($TE_1 + 1.25 \times T_2^0$), and N_2 = 12 (17). The error in the resultant T_2 remains similar over a −25% to +40% range about T_2^0, as shown in Fig. 2 of Ref. 9. This strategy led to a 3.6-h protocol: 55 and 164 min at TE_1 and TE_2.

^{1}H-MRSI Postprocessing

The ^{1}H-MRSI data were processed offline with in-house software. Residual water signals were removed in the time domain, followed by apodization with a 6-Hz Lorentzian filter. Voxel-shift to align the CSI grid with the NAA VOI was followed by Fourier transform in the time and two spatial dimensions (LR, AP) and Hadamard transform along the IS direction. Automatic frequency and zero-order phase corrections were done in reference to the NAA peak in each voxel, as shown in Fig. 1. Relative levels of NAA, Cr, and Cho were estimated from their peak areas using parametric spectral modeling and least-squares optimization, as shown in Fig. 2 (7).

Metabolite T_2 Determination

Proton T_2 relaxation times of the NAA, Cr, and Cho were assessed in vivo in each voxel using,

$$T_2 = (TE_2 - TE_1) / \ln (S_1 / S_2), \quad [1]$$

where S_1 and S_2 are the metabolite's peak areas at the short, TE_1, and long, TE_2, in that voxel. A total of six different structures/regions were examined: the caudate nucleus, thalamus, putamen, and cingulate gyrus in the gray matter (GM); and the splenium of the corpus callosum and centrum semiovale in the white matter (WM). Each was outlined manually on the axial MRI (c.f., Fig. 2) and our software averaged the metabolites' T_2s in all voxels that fell entirely or partially within the outline. No cerebrospinal fluid (CSF) partial volume correction was made to the estimated metabolite levels since its contribution is the same at either TE and cancels out in the S_1/S_2 ratio of Eq. [1].

RESULTS

Sample spectra at the short and long echo times are shown in Figs. 1 and 2. They demonstrate the SNR and spectral resolution obtained at 7T from 64-μl voxels at these TEs. The average metabolite SNRs, defined as peak-height divided by twice the root-mean-square of the noise

(see 4.3.14 in Ref. 19) for the short TE_1 were 9.8 ± 1.0, 10.0 ± 1.0, and 8.9 ± 1.2 (mean ± SEM) for NAA, Cr, and Cho, respectively. Comparison of the spectra at the short and long TEs in Figs. 1 and 2 demonstrate the substantial T_2 weighting incurred. The T_2 values of the regions shown in Fig. 2 and obtained as described above, are compiled in Table 1. Note that the NAA, Cr, and Cho T_2s are similar among the GM and WM regions studied.

The T_2 histograms for the NAA, Cr, and Cho levels from all 320 VOI voxels from each of the four animals studied are shown in Fig. 3. Note the overall histogram shape for each of the three metabolites is similar among the four animals, indicating good interanimal reproducibility.

DISCUSSION

Accurate values for metabolite relaxation times serve two main roles: they are required for reliable and reproducible quantification (10); and they are necessary to establish the optimal sequence acquisition parameters (18). Although several studies have shown that the T_2s of water and metabolites progressively shorten with the increase of B_0, only a few report in vivo values much above 3T (15,16). While they exhibit a consistent trend, the actual metabolite T_2s or the extent of their variations in different macaque brain regions were hereto unknown.

The localization and two-point T_2 techniques yielded in vivo 7T T_2 maps at optimal precision for the available time, over an extensive (25%) of the macaque brain at spatial resolution that scales as the respective brain volumes. The results reveal that these T_2 values are, as expected, much shorter than the 180−250 ms reported for these metabolites at 3T in the human brain (9,10). Comparing with single-voxel human T_2 values at 7T reported by Michaeli et al. (15) shows that these T_2 values are in agreement with the macaque's, i.e., 109 vs. 114 ms for Cr and 158 vs. 169 ms for NAA (Cho T_2 was not reported in that study). This suggests that ultra-high-field T_2s transcend species and that in this respect macaques are good model system for the human brain.

The spatial resolution and extensive coverage (20 cm^3 of the ~80-cm^3 brain) also offer an opportunity to examine two assumptions often made in quantitative ^{1}H-MRSI: that each metabolite has one global T_2; and that it is the same in all subjects. Our results conveniently substantiate both. Specifically, the variation in T_2 values among different regions within the GM or WM is less than 5% for NAA, Cr, and Cho. Such narrow distribution leads to under 5% metabolite concentration estimation variations in the short and intermediate $TE < T_2$, regimes (9).

Although time and cost preclude test-retest experiments to ascertain the intra-animal reproducibility (precision) of these T_2s explicitly, their coefficient of variation (CV) obtainable with this method cannot theoretically be better than $3.6/\mathrm{SNR}_{16}$ (9,17). (SNR_{16} is achieved if the entire duration of the experiment were spent for 4 + 12 = 16 averages at TE_1). This places the lower limit on what the instrumental noise contribution to the CV might be. Since for four averages at TE_1 the SNR_4 were ≈ 10 (see Results) extrapolating to 16 averages renders $\mathrm{SNR}_{16} = \mathrm{SNR}_4 \times \sqrt{16/4} \approx 20$, indicating that the CVs in a single voxel cannot be smaller than $3.6/\mathrm{SNR}_{16} \approx 20\%$.

The actual upper limit on the CV from the combination of instrumental and biological noise is estimated from the ~30% half-width at half-maximum of the histograms in Fig. 3. Assuming that these two noise sources are independent and add as $\mathrm{CV}^2_{\mathrm{total}} = \mathrm{CV}^2_{\mathrm{biology}} + \mathrm{CV}^2_{\mathrm{instrument}}$, we deduce that the biological intra-animal T_2s variability is less than 22%. Since the biological variability is similar in its magnitude to the instrumental contribution in this experiment, comparisons of T_2's in single voxels are unable to provide biologically significant information. Averaging several voxels within a region of interest (ROI) and across several macaques,

however, can substantially reduce the instrumental component of the noise. This is reflected in the T_2s reported in Table 1, where the 3% to 7% CVs are sufficiently small for the reported T_2s to be considered characteristic of "healthy" in this species. This also suggests that additional T_2 measurements on healthy animals, e.g., at study onset, are unnecessary since they are unlikely to yield significantly different results.

It is noteworthy that although a 3.6-h-long protocol may seem excessive, it is merely the consequence of the target spatial resolution and T_2 precision. Since the sensitivity of ^{1}H is not a function of the sample, but only of the voxel size and acquisition time (13), a 10% T_2 precision in a human at 7T and 1-cm^3 voxels will be $(16/3)^2 \approx 25$-fold shorter—a very feasible ~8 min.

CONCLUSIONS

Combining 3D ^{1}H-MRSI with an optimized two-point acquisition protocol makes for the most efficient use of ~4h to estimate regional neurometabolites T_2 in rhesus macaques at spatial resolution proportional to analogous structures in the human brain. These regional T_2 values are in line with the inverse relationship with magnetic field strength and in excellent agreement with the human in vivo values, as indeed expected from a good model system. These T_2s and their variations between several WM and GM structures indicate that for the purposes of metabolic quantification use of one value for each metabolite is sufficient for T_2-weighting corrections for intermediate or longer *TE* sequences at 7T. The narrow, overlapping T_2 histograms for these metabolites indicates that they are likely to be characteristic of "healthy" in this species.

ACKNOWLEDGMENTS

We thank Dr. Andrew Maudsley of the University of Miami for the use of the SITools-FITT spectral modeling software, Ms. Diane Raikowsky and Drs. Mike Duggan and Elisabeth Moeller for animal veterinary care, Mr. Andreas Potthast and Drs. Christopher Wiggins, Graham Wiggins, and Lawrence Wald for 7T technical support. The MGH A.A. Martinos Center for Biomedical Imaging is also supported by the National Center for Research Resources grant number P41RR14075 and the Mental Illness and Neuro-science Discovery (MIND) Institute.

Grant sponsor: National Institutes of Health (NIH); Grant numbers: EB01015, NS050520, NS050041, NS051129, AI028691; Grant sponsor: National Center for Research Resources; Grant number: P41RR14075; Grant sponsor: Mental Illness and Neuroscience Discovery (MIND) Institute.

REFERENCES

1. Greco JB, Westmoreland SV, Ratai EM, Lentz MR, Sakaie K, He J, Sehgal PK, Masliah E, Lackner AA, Gonzalez RG. In vivo 1H MRS of brain injury and repair during acute SIV infection in the macaque model of neuroAIDS. Magn Reson Med 2004;51:1108–1114. [PubMed: 15170829]
2. Roitberg B, Khan N, Tuccar E, Kompoliti K, Chu Y, Alperin N, Kordower JH, Emborg ME. Chronic ischemic stroke model in cynomolgus monkeys: behavioral, neuroimaging and anatomical study. Neurol Res 2003;25:68–78. [PubMed: 12564129]
3. Garcia-Cabezas MA, Rico B, Sanchez-Gonzalez MA, Cavada C. Distribution of the dopamine innervation in the macaque and human thalamus. Neuroimage 2007;34:965–984. [PubMed: 17140815]
4. Jansen JF, Backes WH, Nicolay K, Kooi ME. 1H MR spectroscopy of the brain: absolute quantification of metabolites. Radiology 2006;240:318–332. [PubMed: 16864664]
5. Juchem C, Merkle H, Schick F, Logothetis N, Pfeuffer J. Region and volume dependencies in spectral line width assessed by 1H 2D MR chemical shift imaging in the monkey brain at 7T. Magn Reson Imaging 2004;22:1373–1383. [PubMed: 15707787]
6. Gruetter R, Tkac I. Field mapping without reference scan using asymmetric echo-planar techniques. Magn Reson Med 2000;43:319–323. [PubMed: 10680699]

7. Soher BJ, Young K, Govindaraju V, Maudsley AA. Automated spectral analysis III: application to in vivo proton MR spectroscopy and spectroscopic imaging. Magn Reson Med 1998;40:822–831. [PubMed: 9840826]
8. Dong Z, Dreher W, Leibfritz D. Toward quantitative short-echo-time in vivo proton MR spectroscopy without water suppression. Magn Reson Med 2006;55:1441–1446. [PubMed: 16598735]
9. Zaaraoui W, Fleysher L, Fleysher R, Liu S, Soher BJ, Gonen O. Human brain-structure resolved T(2) relaxation times of proton metabolites at 3 Tesla. Magn Reson Med 2007;57:983–989. [PubMed: 17534907]
10. Tsai SY, Posse S, Lin YR, Ko CW, Otazo R, Chung HW, Lin FH. Fast mapping of the T2 relaxation time of cerebral metabolites using proton echo-planar spectroscopic imaging (PEPSI). Magn Reson Med 2007;57:859–865. [PubMed: 17457864]
11. Cheverud J, Falk D, Vannier M, Konigsberg L, Helmkamp R, Hildebolt C. Heritability of brain size and surface features in rhesus macaques (Macaca mulatta). J Hered 1990;81:51–57. [PubMed: 2332614]
12. Baare W, Hulshoff Pol H, Boomsma D, Posthuma D, de Geus E, Schnack H, van Haren N, van Oel C, Kahn R. Quantitative genetic modeling of variation in human brain morphology. Cereb Cortex 2001;11:816–824. [PubMed: 11532887]
13. Macovski A. Noise in MRI. Magn Reson Med 1996;36:494–497. [PubMed: 8875425]
14. Vaughan JT, Garwood M, Collins CM, Liu W, DelaBarre L, Adriany G, Andersen P, Merkle H, Goebel R, Smith MB, Ugurbil K. 7T vs. 4T: RF power, homogeneity, and signal-to-noise comparison in head images. Magn Reson Med 2001;46:24–30. [PubMed: 11443707]
15. Michaeli S, Garwood M, Zhu XH, DelaBarre L, Andersen P, Adriany G, Merkle H, Ugurbil K, Chen W. Proton T2 relaxation study of water, N-acetylaspartate, and creatine in human brain using Hahn and Carr-Purcell spin echoes at 4T and 7T. Magn Reson Med 2002;47:629–633. [PubMed: 11948722]
16. Otazo R, Mueller B, Ugurbil K, Wald L, Posse S. Signal-to-noise ratio and spectral linewidth improvements between 1.5 and 7 Tesla in proton echo-planar spectroscopic imaging. Magn Reson Med 2006;56:1200–1210. [PubMed: 17094090]
17. Fleysher L, Fleysher R, Liu S, Zaaraoui W, Gonen O. Optimizing the precision-per-unit-time of quantitative MR metrics: Examples for T(1), T(2), and DTI. Magn Reson Med 2007;57:380–387. [PubMed: 17260375]
18. Goelman G, Liu S, Hess D, Gonen O. Optimizing the efficiency of high-field multivoxel spectroscopic imaging by multiplexing in space and time. Magn Reson Med 2006;56:34–40. [PubMed: 16767711]
19. Ernst, RR.; Bodenhausen, G.; Wokaun, A. Principles of nuclear magnetic resonance in one and two dimensions, The International Series of Monographs on Chemistry. Clarendon Press; Oxford: 1987. p. 152

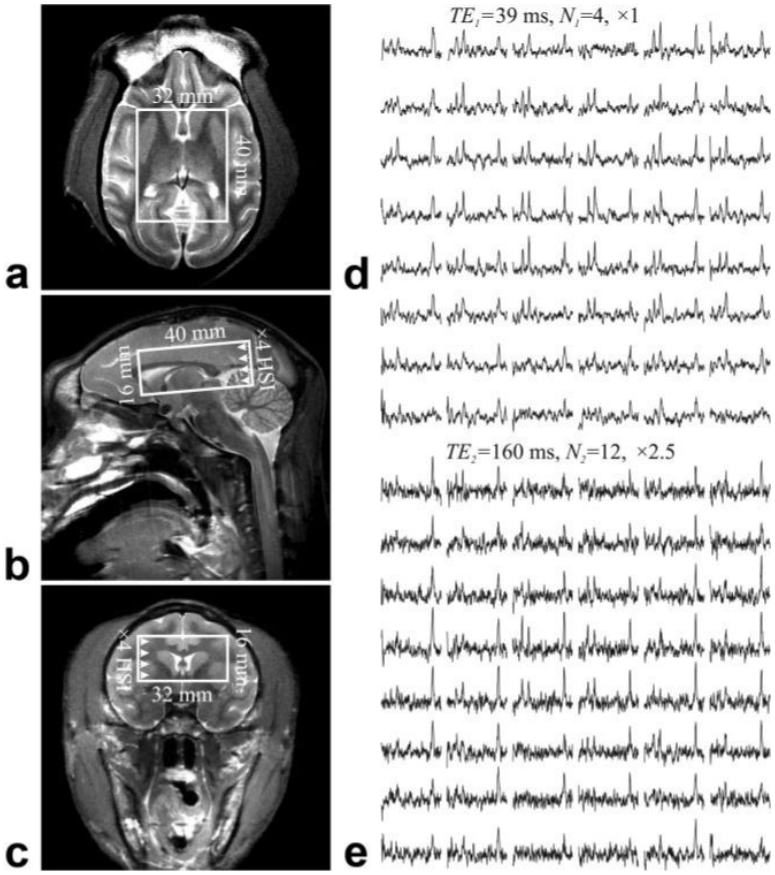

FIG. 1.

Left: (**a**) Axial, (**b**) sagittal, and (**c**) coronal T_2-weighted MRI and typical position of the single-oblique 4.0 × 3.2 × 1.6 cm^3 (AP × LR × IS) VOI in the ~80-cm^3 macaque brain. Right: Axial matrices of the real part of the spectra from the VOI over slice (a), from (**d**) the short TE_1 = 39 ms, N_1 = 4 data set and (**e**) the long TE_2 = 165 ms, N_2 = 12 data set acquisitions. All spectra are on common 3.5− 1.8 ppm and intensity scale at each *TE*. Long *TE* spectra are on a vertical scale × 2.5 times smaller than the short *TE*. Note the spectral resolution and SNR obtained from these isotropic (0.4 cm^3) = 64-μl voxels and the substantial T_2-weighting incurred from (d) to (e).

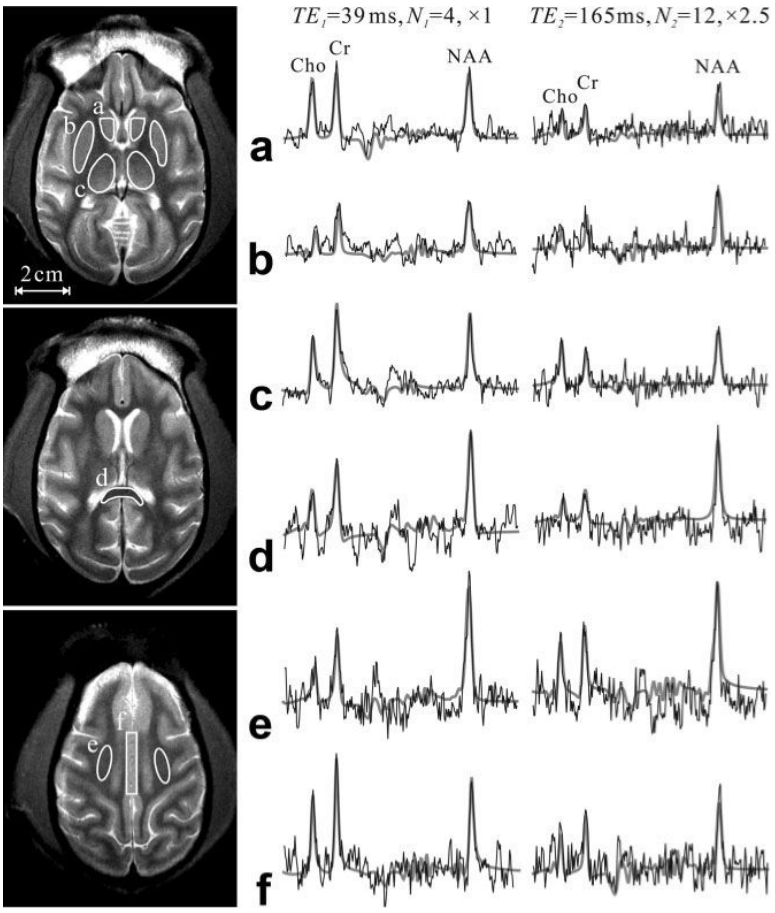

FIG. 2.

Axial brain T_2-weighted images showing the ROIs where the voxels' T_2 were averaged (solid lines): (**a**) caudate nucleus, (**b**)putamen, (**c**) thalamus, (**d**) splenium of the corpus callosum, (**e**) centrum semiovale, and (**f**) cingulate gyrus. Right: Spectra at the two *TE*s from one 64-μl voxel within the each of the corresponding ROIs (thin black line) superimposed with the FITT (7) lineshapes used for T_2 estimation (thick gray lines). Note its good estimate of the experimental spectra at each of the two echo times and the substantial T_2-weighting incurred between them.

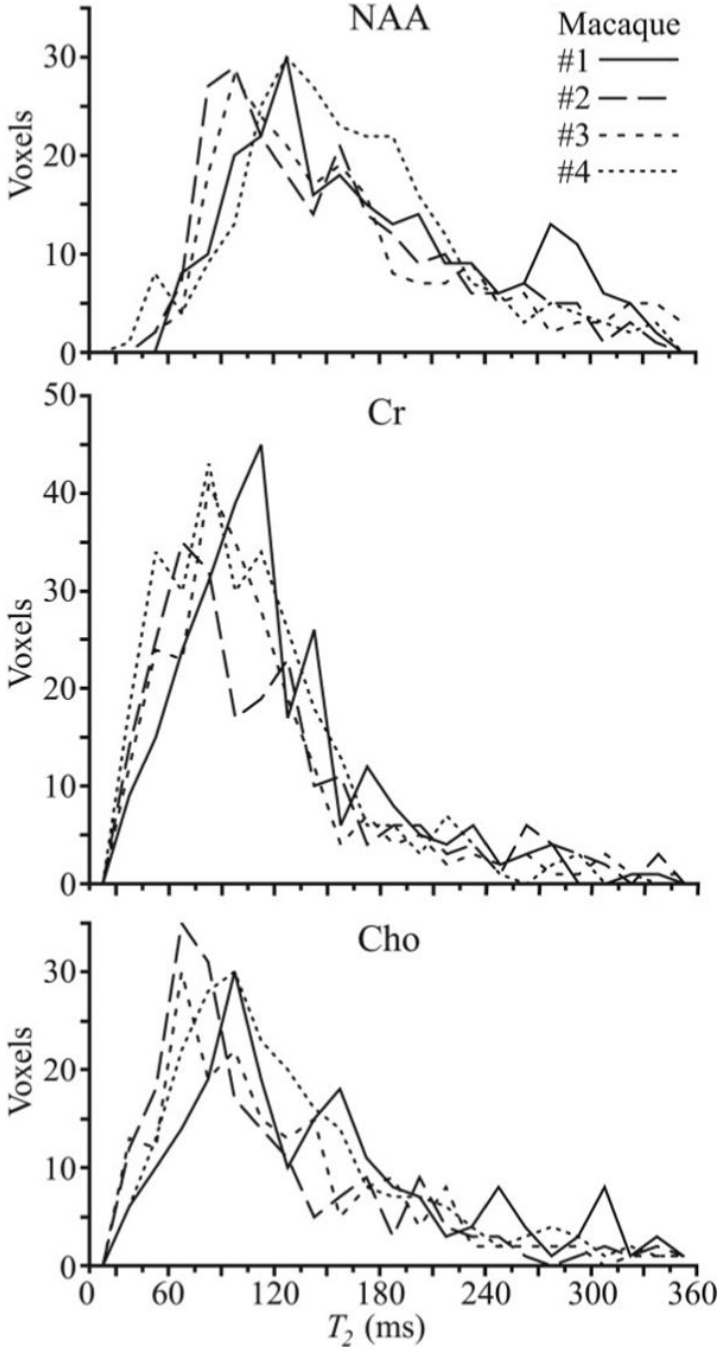

FIG. 3.

Histograms of the NAA, Cr, and Cho T_2s from all 320 voxels in the VOI for each of the four macaques. Note the interprimate similarity of the histograms for each of the metabolites, indicating that: 1) a global T_2 value for each would lead to less than ±10% variation in metabolic quantification; and 2) these T_2 distributions are, therefore, probably characteristic of "healthy" in this species' brain. Note that the histograms peak positions yield T_2 values similar to those reported in the human brain at 7T, making the macaque a good model system in this respect.

Table 1

Mean ± SEM Values of Proton T_2 Relaxation Times (ms) at 7T of *N*-Acetylaspartate (NAA), Creatine (Cr), and Choline (Cho) in the Various GM and WM Brain Regions Shown in Fig. 2, from All Four Macaques Studied

	NAA T_2 (ms)	Cr T_2 (ms)	Cho T_2 (ms)
Gray matter (GM) structures			
Caudate	173 ± 13	109 ± 13	132 ± 16
Thalamus	184 ± 14	118 ± 4	131 ± 8
Putamen	174 ± 12	116 ± 6	122 ± 10
Cingulate gyrus	169 ± 6	126 ± 4	133 ± 3
Average of GM structures	175 ± 3	118 ± 7	129 ± 3
White matter (WM) structures			
Splenium of CC	180 ± 3	112 ± 4	133 ± 8
Centrum semiovale	167 ± 4	119 ± 6	122 ± 5
Average of WM structures	173 ± 6	116 ± 4	127 ± 6
Global WM + GM average	169 ± 2.3	114 ± 1.9	128 ± 2.4

CC = corpus callosum.